Supporting information

For

Elucidating Nano-Cu Interactions in Grapevine Leaves: Formulation-Dependent Foliar Affinity, Uptake, and Leaf Persistence Overtime

Diana Salvador[1], Matheus Miranda[2,3], Sandra Rodrigues[4], Hiram Castillo-Michel[5], Cátia Fidalgo[1], Artur Alves[1], Mickael Wagner[6,7], Camille Larue[7], Sónia M. Rodrigues[4] & Astrid Avellan[6 *]

1. Department of Biology and Centre for Environmental and Marine Studies (CESAM), Universidade de Aveiro, Portugal
2. Institute of Environmental, Chemical and Pharmaceutical Sciences - Federal University of São Paulo, Diadema, Brazil
3. Department of Chemistry and Centre for Environmental and Marine Studies (CESAM), Universidade de Aveiro, Portugal
4. Department of Environment and Planning and Centre for Environmental and Marine Studies (CESAM), Universidade de Aveiro, Portugal
5. European Radiation Synchrotron Facilities, Grenoble, France
6. Géosciences Environnement Toulouse (GET), CNRS, UMR 5563, UT3, IRD, CNES, OMP, France
7. Centre de Recherche sur la Biodiversité et l'Environnement (CRBE), Université de Toulouse, CNRS, IRD, Toulouse INP, Université Toulouse 3 – Paul Sabatier (UT3), France
* corresponding author astrid.avellan@cnrs.fr

1. Materials and methods

Characterization of ChiBSACuO-NPs

1. Zeta potentials of the nanoparticles

The nanoparticle surface charge in different pHs was determined by measuring the particle zeta potentials using a Zetasizer Nano-ZS90 (Malvern Instruments, UK). Briefly, 1 mg of ChiBSACuO-NPs and ChiCuO-NPs were mixed with 10 ml Milli-q water (pH 6.8) and was subjected to 5 min bath Ultrasonic. 1 mL of the suspension was then transferred to a potential zeta cuvette for measurement at 25°C and expressed as an average of 10 readings.

2. Attenuated total reflection-Fourier transform infrared spectroscopy (ATR-FTIR)

FTIR spectroscopy was performed to analyze the nanoparticle surface. Each of the samples was placed onto the diamond ATR window of an Avatar 360 Thermo Nicolet spectrometer and scanned over the range of 400–4000 cm^{-1} with a resolution of 4 cm^{-1} in transmission mode and expressed as an average of 64 readings.

3. X-ray diffraction analysis (XRD)

XRD standards were obtained with Cu-Kα radiation using an Empyrean diffractometer (PANanlytical, The Netherlands). Measurements were made using a step scan program with 0.02° per step and a 5 second acquisition time that was 20 to 80°. XRD data were analyzed using Match 3 (PANanlytical BV Almelo, The Netherlands) for the identification of crystalline phases.

4. Loading efficiency of CuO-NPs

The total copper content in lyophilized powders was determined by Inductively Coupled Plasma Mass Spectrometry (ICP-MS, Thermo-X Series,). Before the ICP-MS analysis, the samples were digested in a microwave heating system (Speedwave 4, Berghef). 10 mg of sample was treated with 1.5 ml of pure HNO_3. The heating program used for acid digestion was: TMAX = 180 °C, ramp time = 5 min, waiting time = 15 min, power = 90 W. Then, the samples were cooled for 30 min at room temperature and the volume was made up to 25 mL of Milli-q water. The measurements were performed in triplicate.

The efficiency percentage loading was determined by the following:

$$Loading\ efficiency = \frac{Mf(g) \times C1(g)}{Mi(g) \times C2(g)} \times 100$$

Loading efficiency Equation. ***Mf*** is the final mass obtained in the synthesis of ChiBSACuO-NPs; ***Mi*** is the initial mass of CuO-NP added to the synthesis; ***C1*** is the concentration of Cu in ChiBSACuO-NPs (Value obtained in by ICP technique); ***C2*** is the concentration of Cu in CuONPs (Value obtained by ICP technique).

5. Dissolution assays

To evaluate the nano-Cu dissolution in DIW, solutions of each Cu treatment were prepared at 1 mg/L and placed in horizontal agitation for 7 days. At 0, 3 and 7 days, two aliquots of 2 mL were collected: one for total Cu analysis and a second, for analysis of the dissolved Cu. The total Cu aliquot was immediately acidified with HNO_3 for ICP-MS analysis while the second aliquot was centrifuged for 30 minutes at 16 000 g, ¼ of the total volume was collected and placed in a new tube, diluted and acidified for ICP-MS analysis. The dissolution % was calculated by the following formula:

$$Dissolution\ \% = \frac{m\ dissolved\ Cu\ (mg)}{m\ total\ Cu\ (mg)} \times 100$$

Plant experiments

Grapevines were grown in pots with a mix of peatmoss and perlite, and watered with ¼ Hoagland Solution without Cu, to limit the Cu supply. Grapevines were not Cu deprived as the substrate where they were grown had Cu in its composition. Each pot had a mass of 0.194 ± 0.008 µg of Cu.

Hoagland Solution

Table S1. Contribution of each macro and micronutrient in the ¼ strength modified Hoagland solution prepared.

Macronutrients	**Concentration (mM)**
KNO_3	1.29
$Ca(NO_3)•4H_2O$	1.20
$MgSO_4•7H_2O$	0.50
KH_2PO_4	0.25
Micronutrients	
NaFe(III)-EDTA	5.00×10^{-3}

H_3BO_3	11.56 x 10^{-3}
$Na_2MoO_4 \cdot 2H_2O$	0.12 x 10^{-3}
$ZnSO_4$	0.19 x 10^{-3}
$MnCl_2$	2.29 x 10^{-3}

Plant exposure

Two leaves per plant were trapped with clothes pin to turn the abaxial side upwards, allowing drop deposition. Abaxial side was chosen for application since grapevines are hypostomatous (1), which could increase the nano-Cu uptake (stomatal route + cuticular route). Four dots, in three different leaf locations, were made using a permanent marker, at the leaf surface to mark the exact location of the drop deposition. Deposition spots were chosen based on the following criteria: (i) avoid vasculature and (ii) choose a leaf spot where the drop could hold steady while the applied drops were drying. Figure S1 demonstrates the prepared setup.

Figure S1 - Setup used for the drop deposition on the abaxial side.

Copper quantification in plant tissues: ICP-MS analysis details

Copper analysis in the extracts was performed by ICP-MS (Agilent 7700 ICP-MS equipped with an octupole reaction system (ORS) collision/reaction cell technology to minimize spectral interferences) using Rhodium (103Rh) as internal standard. The calibration was established with a Certified Reference Material (www.cpachem.com, traceable to NIST), verified with an independent standard (with recoveries between 92 and 104%; average=98%) and check standards were run every 15 samples (with recoveries between 96 and 109%; average=102%). The quantification limit of the instrument was 0.5 µg/L. Instrumental precision of determinations performed in duplicate was always <5%.

Cu standards used in XANES analysis: List and synthesis

CuO-NPs, $CuSO_4$ and $Cu_3(PO_4)_2$ were purchased and prepared for XANES analysis at 1 g of Cu/L prior to the beam time analysis. Cu-alginate, Cu-citrate, Cu-cysteine, Cu-glutathione, Cu-nicotinamide, and ChiBSACuO-NPs were synthesized in the laboratory based on previously published experimental protocols. Detailed description of each Cu standard synthesis is provided below. Synthesis of ChiBSACuO-NPs is detailed in the body of the article in section 2.1.

Table S2. List of synthesized Cu standards used in XANES.

Standard	Type of bond	Reference
Cu-alginate	Cu-O-R	(2)
Cu-citrate	Cu-O-R	(3)
Cu-cysteine	Cu-S-R	(4)
Cu-glutathione	Cu-S-R	(5)
Cu-nicotinamide	Cu-N	(6)
ChiBSACuO-NPs	Cu-O	(7)

Cu-alginate

A mass of 1.0 g of sodium alginate was added to 100 mL of DIW and placed under agitation for 3h, at room temperature. After 3h, this viscous gel is added, drop by drop, to a solution of 2.5 g of $CuSO_4 \cdot 5H_2O$ dissolved in 250 mL. The mixture was then left in low agitation for 2h. After 6h, the resulting blue Cu-alginate beads were then washed in DIW and placed to dry at 40°C overnight.

Cu-citrate

Cu-citrate was synthesized in a 1:1 ratio. 2.94 g of $Na_3C_6H_5O_7 \cdot 2H_2O$ was dissolved in 50 mL and a solution of $CuSO_4 \cdot 5H_2O$ was prepared. The mixture was left in agitation and after 1h a precipitate was formed. A powder was obtained after vacuum filtration and drying the mixture overnight. Cu-citrate was kept in a desiccator until usage.

Cu-cysteine

Synthesis of Cu-cysteine was based on Dokken et al. protocol with some modifications. A mole ratio of 1:6 of Cu:cysteine was used for this synthesis and the mixture was prepared for a final concentration of 1 g of Cu/L. Briefly, L-cys was dissolved in 50 mL ethanol and $CuCl_2 \cdot 2H_2O$ was added to the mixture and left in agitation at 30°C. After a pale pink precipitate formed, the Cu-cysteine mixture was obtained by vacuum filtration and dried overnight at 40°C. A final mass of 4.5 mg of Cu-cysteine was obtained and stored protected from the light.

Cu-glutathione

Cu-glutathione was synthesized by adding 4 mmol of glutathione (M=307.32 g/mol) to 20 mL of DIW. Then, 20 mL of $CuCl_2 \cdot 2H_2O$ solution was prepared at 1 mmol (M=170.48 g/mol) and both solutions were mixed. After addition of $CuCl_2 \cdot 2H_2O$ solution, the mixture became cloudy and was left for agitation. At this point, pH was adjusted (increased) to 4 with NaOH at 5M and the mixture turned into a translucid yellow. DIW was added to a final volume of 50 mL and the Cu-glutathione mixture was kept in a closed vial, protected from the light, for a week. After this period, the mixture was dark blue.

Cu-nicotinamide

Cu-nicotinamide was synthesized based on Baig et al. protocol with small changes. This synthesis was performed with $CuCl_2 \cdot 2H_2O$ and nicotinamide (M=122.12 g/mol) in a 2:5 ratio. A solution of $CuCl_2 \cdot 2H_2O$ and a solution of nicotinamide at 0.1 M were prepared, at room temperature. Both

solutions were mixed, and crystals were formed. The supernatant was removed, and the crystals were dried at 40°C overnight.

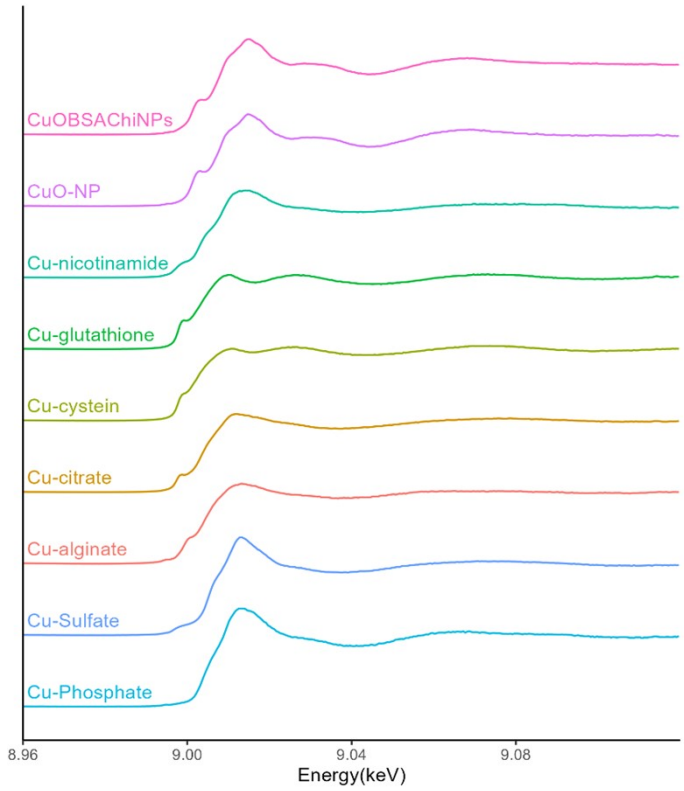

Figure S2 – XANES standards analyzed at the beamline ID-21.

Pipetting error test

To evaluate if the recovered copper could be affected by pipetting errors, a control of deposition was performed. Briefly, for each treatment, 6 drops of 40 µL were added to a 50 mL tube (the same volume added to one plant), in triplicates. Then, 200 µL of HNO_3 65% was added to the tubes and left to react overnight. The next day the control deposition samples were diluted with dH_2O to have a final HNO_3 of 1% for ICP-MS analysis. Initial suspensions/solutions were also analyzed by ICP-MS to assess the proper initial Cu concentration.

The percentage of applied Cu was calculated by dividing the Cu quantified in the control deposition tubes by the Cu in the initial suspension/solutions. The results are presented in Table S3. In this test, we could observe that in CuO-NPs samples, the applied Cu mass was 80.15±4.24% of the theoretical mass, comparing to 97.33±2.86% and 106.72±0.49% from ChiBSACuO-NPs and $CuSO_4$ samples, respectively.

Table S3. Results of the pipetting error test. Cu masses quantified by ICP-MS are presented in µg.

Copper treatment	Cu in the initial suspension/solution (µg)	Cu in the control deposition tubes (µg)	Standard Deviation (µg)	% Applied Cu
CuO-NPs	23.071	18.491	0.978	80.148
ChiBSACuO-NPs	24.502	23.849	0.700	97.332
$CuSO_4$	24.762	26.428	0.123	106.724
MQ	0.000	0.013	0.009	

Total recovered Cu

Quantification of total recovered Cu are presented in mass of Cu (µg), per Cu treatment for both exposure periods, 7 and 25 days (Fig. S3). Contribution from the DIW control was removed from the presented results. Cu recovered from the $CuSO_4$-exposed plants was 95.29±2.55% and 82.43±0.96%, for 7 and 25 days of exposure, respectively. Copper recovered from plants exposed to ChiBSACuO-NPs was 114.76±25.77% for the 7 days-exposed plants and 109.08±9.06% for the 25 days-exposed plants. Regarding the CuO-NP deposition, only 66.83±5.55% and 57.62±12.59% of Cu was recovered after 7 and 25 days of exposure, respectively. CuO-NPs-exposed plants received a lower Cu mass compared to the theoretical Cu mass (26.4 µg) due to the colloidal stability of the suspension. Total Cu in the DIW control plants was 5.33±1.76 µg and 9.46±0.88 µg, for 7 and 25 days of exposure, respectively.

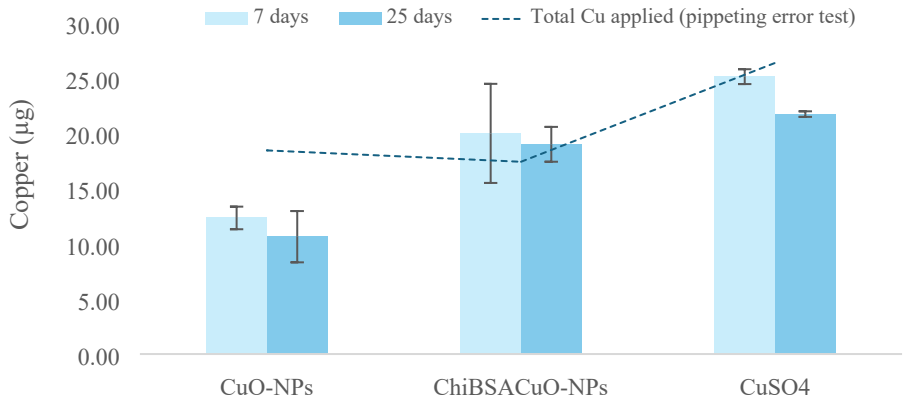

Figure S3 - Total recovered copper (µg) for all copper treatments and two exposure periods.

2. Results

ChiBSACuO-NPs characterization

The ChiBSACuO-NPs present high aggregation properties. Consequently, the hydrodynamic diameter would give an unrealistic value. Therefore, the material was characterized based on the techniques mentioned in the main article.

EDS

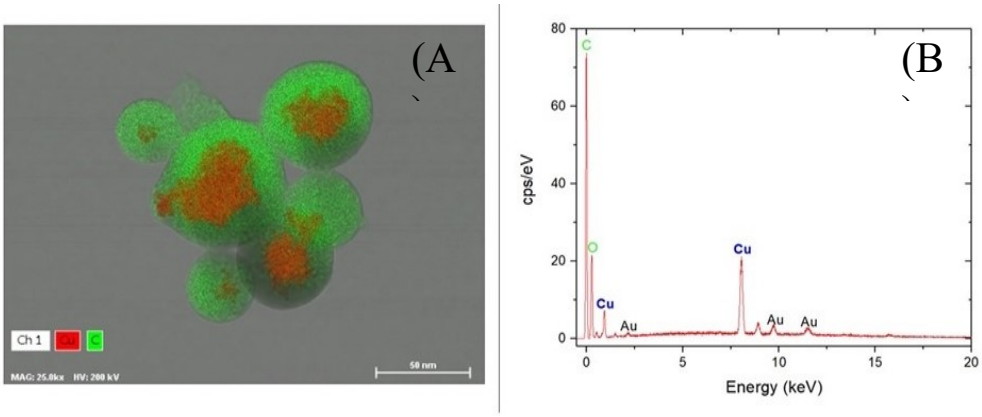

Figure S4 – TEM-EDS analysis of ChiBSACuO-NPs with (A) mapping micrograph (Cu-red, C- green) and (B) EDS spectrogram.

XRD

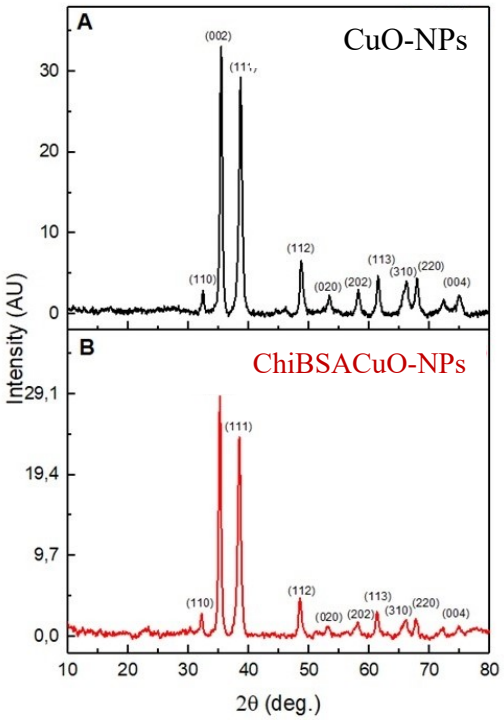

Figure S5 - Diffractograms of (A) Commercial CuO-NPs and (B) ChiBSACuO-NPs.

FTIR

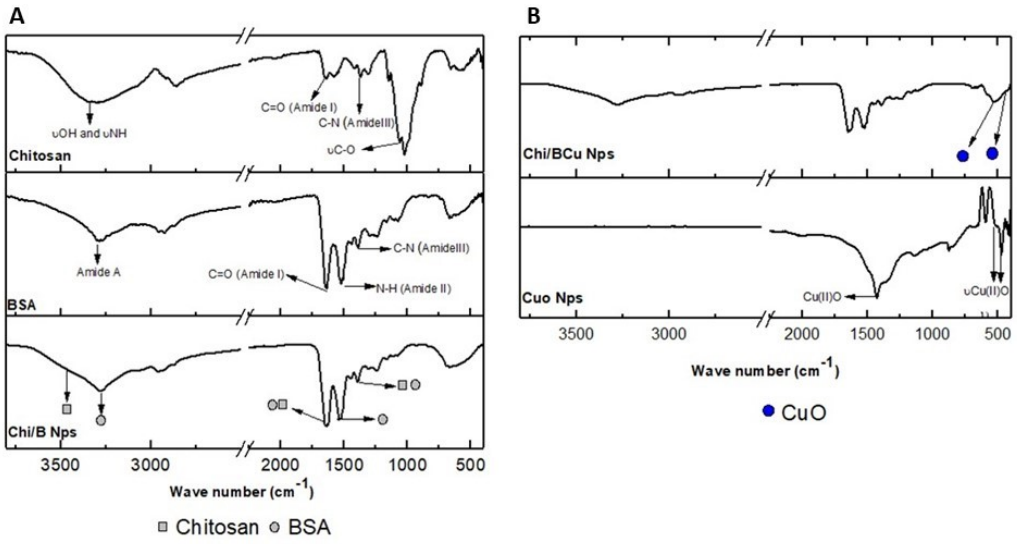

Figure S6 – FT-IR spectrum comparison: (A) Chitosan powder, BSA powder and ChiBSA-NPs (Chi/B Nps in the graph) and (B) CuO-NPs and ChiBSACuO-NPs (Chi/BCuNps in the graph).

Table S4 – ChiBSACuO-NPs and CuO-NPs dissolution tests in DIW. Cu dissolution in % is presented along with the standard deviation.

	ChiBSACuO-NPs		CuO-NPs	
Days	Dissolution (%)	St. Dev (%)	Dissolution (%)	St. Dev (%)
0	1.60	0.429	1.92	0.147
3	6.94	0.945	16.73	1.950
7	12.98	2.192	42.78	6.911

<u>Exposed leaves lesions and correlation with Cu-glutathione speciation in the vasculature</u>

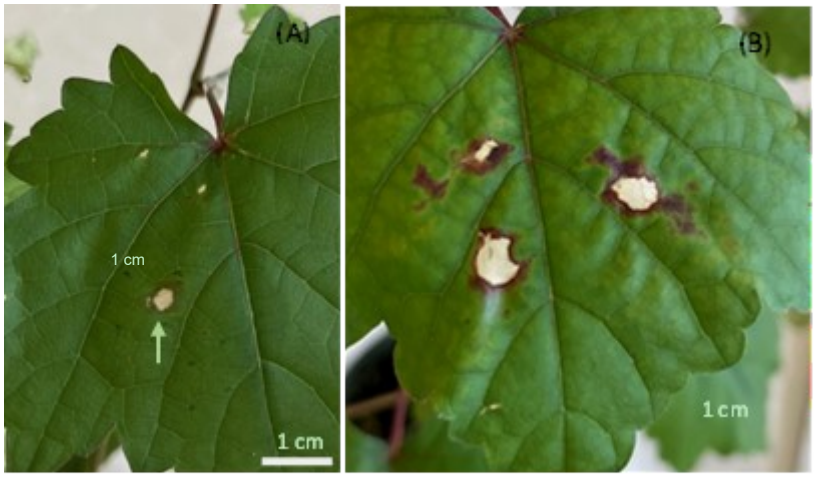

Figure S7 - (A) Lesion in the $CuSO_4$-exposed leaf after 7 days *and (B*) Several lesions observed at a $CuSO_4$-exposed leaf after 25 days.

Cu detected in the mesophyll

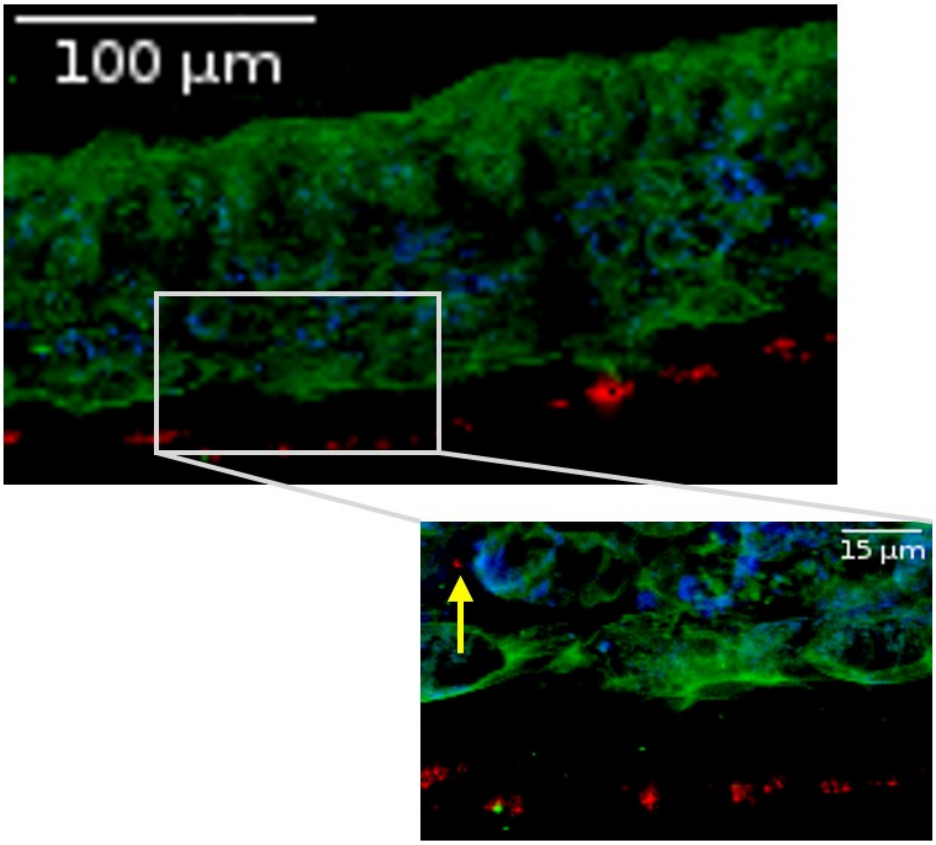

Figure S8 - µ-XRF maps of ChiBSACuO-NPs after 25 days of exposure, highlighting the Cu hotspots in the mesophyll for this foliar treatment, in a higher resolution map. The elements represented are Cu (red), Ca (green) and K (blue). Yellow arrows point at the Cu hotspot in the mesophyll.

Cu translocation to non-exposed tissues

Results of XANES analysis of nano-Cu-exposed petiole samples

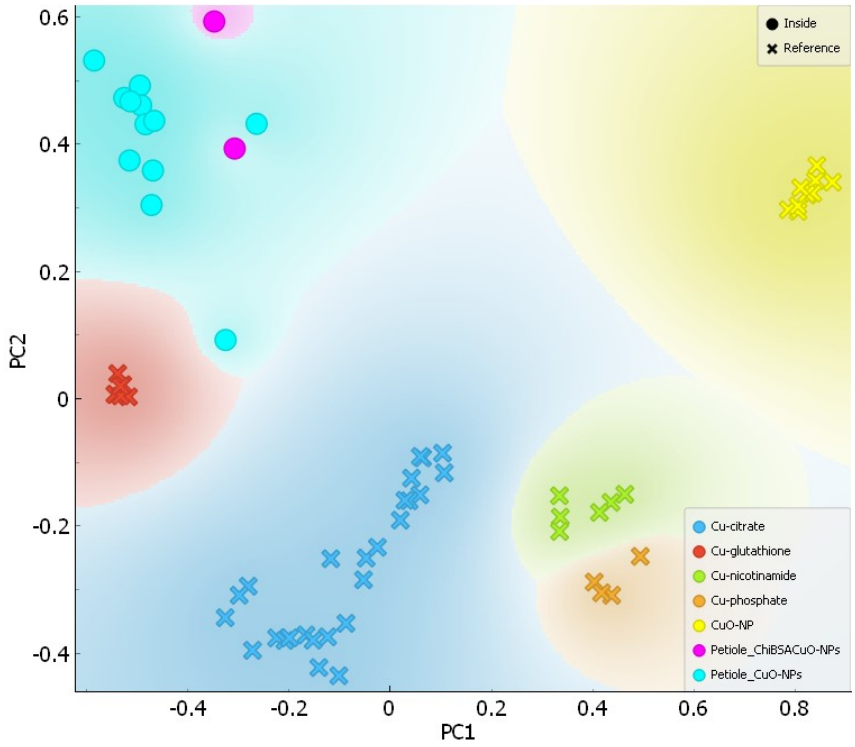

Figure S9 – PCA analysis of µ-XANES spectra obtained on the petiole samples exposed to nano-Cu. ChiBSACuO-NPs are represented in pink, and CuO-NPs are represented in turquoise.

Copper quantified in non-exposed tissues

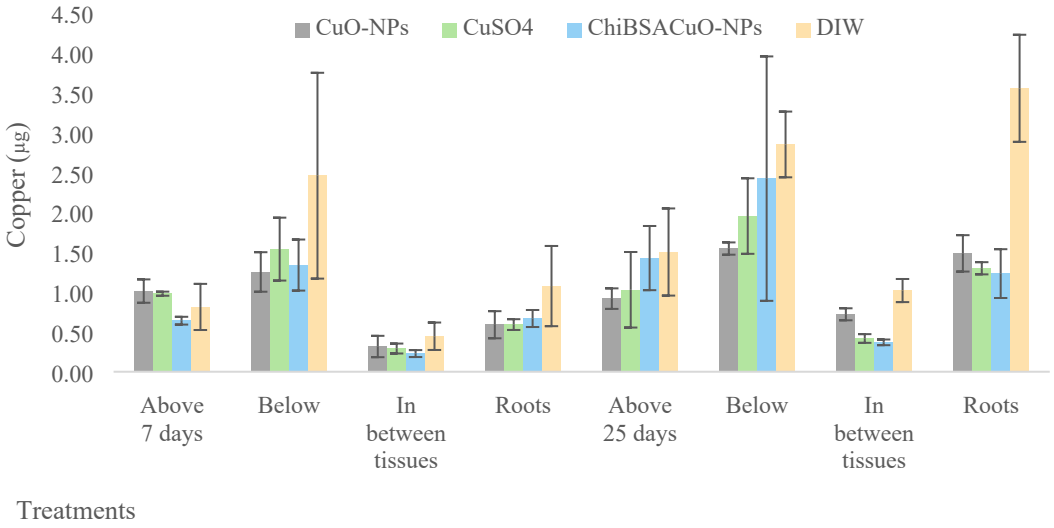

Figure S10 - Copper quantified in the non-exposed tissues, namely tissues above, in between and below the exposed leaves. Results are presented in mass of Cu (µg). There are no significant differences among treatments for the same plant tissue and time of exposure.

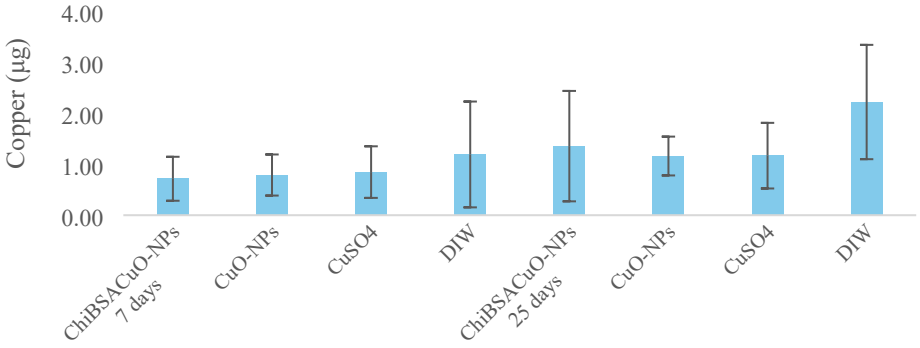

Figure S11 – Total copper (µg) quantified in the non-exposed tissues (tissues above + in between + below the exposed leaves) for each treatment. Statistical analysis was performed using Kruskal-Wallis followed by pairwise Dunn test with Bonferroni p-value correction. There are no significant differences among treatments for the same plant tissue and time of exposure.

References:

1. Keller M. The Science of Grapevines: Anatomy and Physiology [Internet]. Second edi. The Science of Grapevines. Elsevier Science & Technology; 2015. 522 p. Available from: http://ezproxy.umng.edu.co:2048/login?url=https://www.proquest.com/books/science-grapevines/docview/2134393489/se-2?accountid=30799

2. Elhoudi M, Oukhrib R, A. Celaya C, G. Araiza D, Abdellaoui Y, Barra I, et al. Comparison of green bio-based cerium/alginate vs. copper/alginate beads: a study of vibrational and thermal properties using experimental and theoretical methods. J Mol Model [Internet]. 2022;28(2):37. Available from: https://doi.org/10.1007/s00894-022-05028-8

3. Education R. Preparation of copper(II) citrate [Internet]. Available from: https://edu.rsc.org/download?ac=12719

4. Dokken KM, Parsons JG, McClure J, Gardea-Torresdey JL. Synthesis and structural analysis of copper(II) cysteine complexes. Inorganica Chim Acta [Internet]. 2009;362(2):395–401. Available from: https://www.sciencedirect.com/science/article/pii/S0020169308003319

5. Yin SN, Liu Y, Zhou C, Yang S. Glutathione-Mediated Cu(I)/Cu(II) Complexes: Valence-Dependent Effects on Clearance and In Vivo Imaging Application. Nanomaterials [Internet]. 2017;7(6). Available from: https://www.mdpi.com/2079-4991/7/6/132

6. Baig RBN, Vaddula BR, Nadagouda MN, Varma RS. The copper–nicotinamide complex: sustainable applications in coupling and cycloaddition reactions. Green Chem [Internet]. 2015;17(2):1243–8. Available from: http://dx.doi.org/10.1039/C4GC02047B

7. Li Y, Song H, Xiong S, Tian T, Liu T, Sun Y. Chitosan-stablized bovine serum albumin nanoparticles having ability to control the release of NELL-1 protein. Int J Biol Macromol [Internet]. 2018;109:672–80. Available from: http://dx.doi.org/10.1016/j.ijbiomac.2017.12.104